FFT-based trellis receiver for SEFDM signals

Andrey Rashich, Alexandr Kislitsyn, Fadeev Dmitrii, Ngoc Tan Nguyen
Radio and telecommunication systems department
Peter the Great St. Petersburg Polytechnic University
St. Petersburg, Russia
rashich@cee.spbstu.ru

***Abstract*— A new FFT-based trellis receiver for multicarrier signals with nonorthohgonal frequency spacing (spectrally efficient frequency division multiplexing, SEFDM) is proposed. It is based on FFT and max-log-MAP algorithm, which is adapted to work with frequency samples of received signal. The iterative version of demodulator is also developed. The performance of proposed iterative QPSK-SEFDM demodulation is comparable with the one of classic coded QPSK modulation while the spectral efficiency remains very high. The proposed algorithms can demodulate SEFDM signals with large number of subcarriers.**

Keywords—OFDM, NOFDM, BEFDM, SEFDM, multicarrier FTN, iterative receiver, MAP algorithm, 5G

I. INTRODUCTION

At the present time close attention is paid to the 5th generation wireless systems (5G). A lot of research is being done to determine modulation schemes for 5G. One of the possible approaches is the OFDM-signals extension towards nonorthogonal frequency spacing – spectrally efficient frequency division multiplexing (SEFDM) which is a kind of faster-than-Nyquist (FTN) signals. This kind of signals has very high spectral efficiency and the potential benefits from OFDM but is poor for reception: the energy loss is extremely high relative to OFDM.

A number of works addresses the problem of SEFDM reception. The known approaches are successive interference cancellation [2,3], spherical decoder [4] and matched filtering [3,4]. These can be combined with interleaver and forward error correction (FEC) schemes in iterative receiver sometimes providing good results at the cost of extremely high computational complexity. In this paper we propose the asymptotically optimal algorithm for SEFDM demodulation which works with spectral samples. It provides quite good performance for low levels of SEFDM compression without any FEC and shows excellent performance in iterative version with a few number of iterations even for high levels of compression. The BER performance of proposed iterative SEFDM demodulation is comparable with the one of coded orthogonal modulation. The important note is that the normal for OFDM receiver fast Fourier transform FFT block is retained.

The remainder of this paper is structured as follows: the system model description in section II, proposed SEFDM demodulator in section III and its iterative version in section IV. In section V simulation results are presented. Section VI concludes this paper.

II. SYSTEM MODEL

We consider baseband SEFDM-symbols with duration T of the following form:

$$s(t) = \sum_{k=-N/2}^{N/2-1} C_k e^{j\omega_k t} = \sum_{k=-N/2}^{N/2-1} C_k e^{j2\pi k\Delta f t},\ t \in [0; T]. \qquad (1)$$

It is a multicarrier signal with N subcarriers, complex modulation symbols C_k on each subcarrier (QPSK, QAM-16, etc.) with no cyclic prefix. The frequency spacing between adjacent subcarriers is Δf and $\omega_k = 2\pi k\Delta f$. For SEFDM $\Delta f = \alpha/T$, where $\alpha < 1$ is the subcarrier frequency spacing normalized to $1/T = \Delta f_{\text{OFDM}}$, α is a rational number. For OFDM $\alpha = 1$. The subcarrier components of OFDM- and SEFDM-signals for $N = 12$ are shown on Fig. 1.

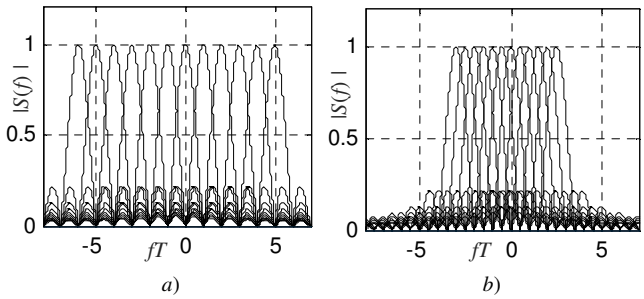

Fig. 1. Spectral representation of OFDM ($\alpha = 1$) (a) and SEFDM signals ($\alpha = 1/2$) (b), $N = 12$

SEFDM-signals occupy less bandwidth than OFDM-signals for the same number of subcarriers, coding rate and modulation type, providing the same data rate. The penalty for this improvement is BER degradation due to interference between the subcarriers in SEFDM. They are not orthogonal as those in OFDM. Throughout this paper a number of side subcarriers in SEFDM is used as guard interval (with zero amplitudes) to prevent aliasing. Thus the full number of subcarriers in SEFDM-signal is N_{full} and the number of used subcarriers (with non-zero amplitudes) is N.

The signal processing is done in digital domain (by FPGAs, DSPs or ASICS) thus we consider the discrete version of SEFDM signals given sampling frequency F_s:

$$s_n = \sum_{k=-N_{full}/2}^{N_{full}/2-1} C_k e^{j2\pi kn\Delta f/F_s} = \Big|_{F_s = N_{full}\Delta f} = \sum_{k=-N_{full}/2}^{N_{full}/2-1} C_k e^{j2\pi kn/N_{full}} \qquad (2)$$

Here $n = 0,\ldots,L-1$, L is the number of time samples in one SEFDM-symbol, $L = F_s T$,. $L = N_{full}\alpha$ if sampling frequency is chosen as $F_s = N_{full}\Delta f$.

The received signal $r(t)$ is corrupted with additive white Gaussian noise (AWGN) $w(t)$:

$$r(t) = s(t) + w(t),\ t \in [0; T]. \quad (3)$$

Sampled version of received signal is the sum of SEFDM samples and AWGN samples:

$$r_n = s_n + w_n,\ n = 0,1,...,L-1. \quad (4)$$

Given the sequence $\{r_n\}_{n=0}^{L-1}$ of received signal samples, we have to get the estimates of transmitted complex modulation symbols $\{\hat{C}_k\}_{k=-N/2}^{N/2-1}$ or channel bits.

The most important thing of OFDM processing is IFFT/FFT usage for signal generation and reception. What we want for SEFDM processing is to keep IFFT/FFT blocks as in OFDM schemes. In other words, the ideal case for us is to use well-studied OFDM generation and reception schemes with minor additions at transmitter side and additional SEFDM demodulation block at the receiver side. In our work we use the first algorithm proposed in [1] to generate SEFDM-symbol and corresponding reverse operations to get spectral samples $\{R_m\}_{m=-N_{FFT}/2}^{N_{FFT}/2-1}$ of SEFDM-symbol at the receiver side (Fig. 2). IFFT at transmitter and FFT at receiver are both of N_{FFT} size. Thus $N_{full} = N_{FFT} = 2^p$, where p is natural. The key role in the reception scheme plays SEFDM-demodulator (gray block in Fig. 2b). It has to correct the interference between the subcarriers and provide the estimates of transmitted modulation symbols (or channel bits). We have to notice that all white blocks in Fig.2 are common to OFDM (except ignoring some samples in modulator and zero insertion in demodulator that are trivial operations).

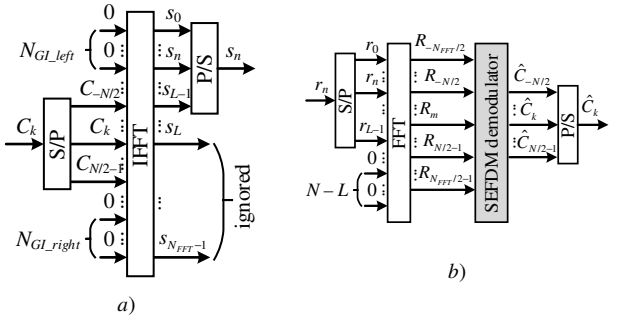

Fig. 2. a) IFFT-based SEFDM modulator; b) FFT-based SEFDM demodulator

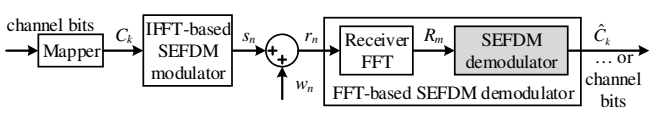

Fig. 3. System model

The considered system model is presented on Fig. 3. It consists of serial concatenation of a mapper, IFFT-based SEFDM modulator, discrete AWGN channel and FFT-based SEFDM demodulator. The latter comprises N_{FFT}-point FFT block and SEFDM demodulator. The mapper associates groups of D channel bits with complex modulation symbols from a particular constellation (ex. QPSK, QAM-16, QAM-64, etc.) with alphabet size $M = 2^D$. IFFT-based SEFDM modulator transforms these symbols into L time samples of SEFDM-symbol. At the receiver side the FFT block generates N_{FFT} frequency samples from received noisy observation time samples of SEFDM-symbol. At last, SEFDM demodulator provides the estimates of transmitted modulation symbols or channel bits.

III. Proposed SEFDM demodulator

We start with considering the discrete channel from the input of IFFT based SEFDM modulator to the output of receiver FFT (Fig. 3). Such discrete channel takes N complex modulation symbols $\{C_k\}_{k=-N/2}^{N/2-1}$ on its input and provides N_{FFT} spectral samples $\{R_m\}_{m=-N_{FFT}/2}^{N_{FFT}/2-1}$ on its output. Based on Fig. 3 and from (2) and (4) we can write the following:

$$R_m = \sum_{n=0}^{L-1} r_n e^{-j2\pi\frac{nm}{N_{FFT}}} = \sum_{k=-N_{FFT}/2}^{N_{FFT}/2-1} \frac{C_k}{N_{FFT}} \sum_{n=0}^{L-1} e^{j2\pi\frac{n(k-m)}{N_{FFT}}} + w_m^{IFFT}. \quad (5)$$

Here $w_m^{IFFT} = \mathrm{IFFT}\left\{\{w_n\}_{n=0}^{L-1}\right\}$. The scaling factor $1/N_{FFT}$ comes from the IFFT block used for SEFDM generation. Assuming no AWGN, we can write the following expression for m-th spectral sample at the receiver FFT output:

$$R_m = \sum_{k=-N_{FFT}/2}^{N_{FFT}/2-1} C_k g_{k,m},\ g_{k,m} = \frac{1}{N_{FFT}} \sum_{n=0}^{L-1} e^{j2\pi n(k-m)/N_{FFT}}.,\quad (6)$$

In (5) and (6) $k, m = -N_{FFT}/2,\ldots,N_{FFT}/2 - 1$. We can see that m-th spectral sample R_m is a linear combination of all the transmitted modulation symbols. The coefficients $g_{k,m}$ introduce the *intersubcarrier* interference, caused by SEFDM modulation (Fig. 4).

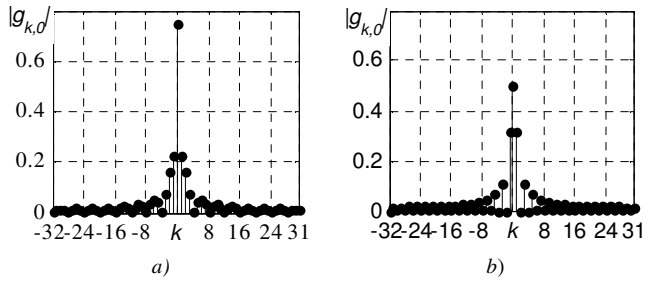

Fig. 4. Absolute values of $g_{k,0}$ for $N_{FFT} = 64$: a) $\alpha = 3/4$; b) $\alpha = 1/2$

Nevertheless, the major effect on the R_m is provided by m-th subcarrier with modulation symbol C_m and the nearest subcarriers with numbers $(m \pm 1)$, $(m \pm 2)$ and so on depending

on α (Fig. 4). In this way, we can consider only a small number K of nearest to position m subcarriers in (6) to compute R_m. Also note that $g_{k,m}$ actually depends only on the difference $(k - m)$. The set of coefficients $g_{k,m}$ is the same for all R_m. So, in (6) we can omit index m in $g_{k,m}$ and simply use g_k, $k = -(K-1)/2, \ldots, (K-1)/2$. Now we can write the following approximation, which is as better as K increases towards N:

$$R_m \approx \sum_{k=-(K-1)/2}^{(K-1)/2} C_k g_k \,. \qquad (7)$$

For example for $N = 64$, $\alpha = 3/4$ and $K = 3$ (only 1 nearest subcarrier is considered on both sides of m-th subcarrier) $g_k = \{-0{,}15 - 0{,}17j;\ 0{,}75;\ -0{,}15 + 0{,}17j\}$.

We can interpret (7) as a linear filter with coefficients g_k, $k = -(K-1)/2, \ldots, (K-1)/2$. This frequency domain filter associates an output sequence $\{R_m\}_{m=-N_{FFT}/2}^{N_{FFT}/2-1}$ with an input sequence $\{C_k\}_{k=-N_{FFT}/2}^{N_{FFT}/2-1}$ (Fig. 5). Here we consider $C_k = 0$ for $k = -N_{FFT}/2, \ldots, -N/2 - 1, N/2, \ldots, N_{FFT}/2 - 1$ (frequency guard intervals).

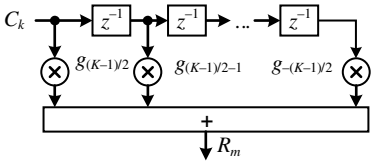

Fig. 5. Filter generation of spectral samples

Note that filter on Fig. 5 includes IFFT-based SEFDM modulator and receiver FFT block. Such a filter produces frequency domain samples of SEFDM-signal. Generally speaking, the filter on Fig. 5 is a finite state machine (FSM). It is convenient to represent it with state transition and output tables. The examples of those for SEFDM with $N = 64$, $K = 3$, $\alpha = 3/4$ and QPSK modulation are presented in tables 1, 2. The bit mapping scheme is the following: {bin'00 = dec'0→ $(1 + 1j)$; bin'01 = dec'1→ $(1 - 1j)$; bin'10 = dec'2→ $(-1 + 1j)$; bin'11 = dec'3→ $(-1 - 1j)$}.

TABLE I. STATE TRANSITION TABLE FOR SEFDM FSM, QPSK, $K = 3$

State name	Filter content	Input symbol			
		dec'0	*dec'1*	*dec'2*	*dec'3*
st_0	dec'00	st_0	st_4	st_8	st_{12}
st_1	dec'01	st_0	st_4	st_8	st_{12}
st_2	dec'02	st_0	st_4	st_8	st_{12}
st_3	dec'03	st_0	st_4	st_8	st_{12}
st_4	dec'10	st_1	st_5	st_9	st_{13}
st_5	dec'11	st_1	st_5	st_9	st_{13}
st_6	dec'12	st_1	st_5	st_9	st_{13}
st_7	dec'13	st_1	st_5	st_9	st_{13}
st_8	dec'20	st_2	st_6	st_{10}	st_{14}
st_9	dec'21	st_2	st_6	st_{10}	st_{14}
st_{10}	dec'22	st_2	st_6	st_{10}	st_{14}
st_{11}	dec'23	st_2	st_6	st_{10}	st_{14}
st_{12}	dec'30	st_3	st_7	st_{11}	st_{15}
st_{13}	dec'31	st_3	st_7	st_{11}	st_{15}
st_{14}	dec'32	st_3	st_7	st_{11}	st_{15}
st_{15}	dec'33	st_3	st_7	st_{11}	st_{15}

TABLE II. OUTPUT TABLE FOR SEFDM FSM, QPSK, $K = 3$, $\alpha = 3/4$, $N = 64$

State name	Input symbol			
	dec'0	*dec'1*	*dec'2*	*dec'3*
st_0	0,45 + 0,45j	0,45 – 1,05j	–1,05 + 0,45j	–1,05 – 1,05j
st_1	0,11 + 0,75j	0,11 – 0,75j	–1,39 + 0,75j	–1,39 – 0,75j
st_2	0,75 + 0,78j	0,75 – 0,72j	–0,75 + 0,78j	–0,75 – 0,72j
st_3	0,42 + 1,08j	0,42 – 0,42j	–1,08 + 1,08i	–1,08 – 0,42i
st_4	0,78 + 0,75i	0,78 – 0,75i	–0,72 + 0,75i	–0,72 – 0,75i
st_5	0,45 + 1,05i	0,45 – 0,45i	–1,05 + 1,05i	–1,05 – 0,45i
st_6	1,08 + 1,08i	1,08 – 0,42i	–0,42 + 1,08i	–0,42 – 0,42i
st_7	0,75 + 1,39i	0,75 – 0,11i	–0,75 + 1,39i	–0,75 – 0,11i
st_8	0,75 + 0,11i	0,75 – 1,39i	–0,75 + 0,11i	–0,75 – 1,39i
st_9	0,42 + 0,42i	0,42 – 1,08i	–1,08 + 0,42i	–1,08 – 1,08j
st_{10}	1,05 + 0,45j	1,05 – 1,05j	–0,45 + 0,45j	–0,45 – 1,05j
st_{11}	0,72 + 0,75j	0,72 – 0,75j	–0,78 + 0,75j	–0,78 – 0,75j
st_{12}	1,08 + 0,42j	1,08 – 1,08j	–0,42 + 0,42j	–0,42 – 1,08j
st_{13}	0,75 + 0,72j	0,75 – 0,78j	–0,75 + 0,72j	–0,75 – 0,78j
st_{14}	1,39 + 0,75j	1,39 – 0,75j	–0,11 + 0,75j	–0,11 – 0,75j
st_{15}	1,05 + 1,05j	1,05 – 0,45j	–0,45 + 1,05j	–0,45 – 0,45j

The filter on Fig. 5 can be regarded as a Markov process. For such a process the probability to be in a certain state at sample k depends only on the state at previous sample $(k - 1)$. The problem of the estimation of state sequence for Markov process is solved by MAP algorithm (usually its log-MAP or MAX-log-MAP versions) [5]. It is widely used as component decoder in iterative decoders of turbo codes and turbo equalizers [6].

Further in this paper the MAP algorithm is adapted to demodulate SEFDM-symbols using spectral samples $\{R_m\}_{m=-N_{FFT}/2}^{N_{FFT}/2-1}$ at the receiver. Given the received frequency samples R_m and (for generality) channel bit a priori LLR's SEFDM demodulator has to provide channel bit a posteriory LLRs. In other words, it has to perform demodulation and demapping tasks. The channel bit LLR for bit u is written in the following way:

$$LLR(u) = \ln \frac{P(u=0)}{P(u=1)} \,. \qquad (8)$$

The MAP algorithm consists of brunch metric calculation, forward and backward recursions and final bit (or symbol) a posteriori probabilities calculation. The extrinsic information is also evaluated in iterative schemes [5].

For SEFDM the brunch metric $\gamma_i(st_p, st_j)$ is associated with a transition between states st_p and st_j for trellis step i. It is a function of received frequency sample and available a priory information for it. The brunch metric in logarithmic domain is evaluated in the following way [6]:

$$\gamma_i(st_p, st_j) = -\frac{1}{\sigma^2}\left(R_i - \sum_{k=-(K-1)/2}^{(K-1)/2} C_{i-k}^{p,j} g_k\right)^2 + \ln P_a(C_i) \,. \quad (9)$$

The symbols $C_{i-k}^{p,j}$ are associated with the pair of states st_p and st_j The second term in (9) is the logarithm of a priori probability of i-th modulation symbol. Given the a priori LLRs

for T channel bits corresponding to the i-th modulation symbol it is straightforward to get all the possible values of $\ln P_a(C_i)$. E. g., for QPSK each modulation symbol corresponds to a pair of bits. Given the a priori LLRs L_x and L_y for the first and the second bits, we can write the following:

$$\ln P_{\text{dec'0}} = L_x + L_y; \ln P_{\text{dec'1}} = L_x; \ln P_{\text{dec'2}} = L_y; \ln P_{\text{dec'3}} = 0 \quad (10)$$

In (10) the term $-\ln((1+\exp(L_x))(1+\exp(L_y)))$ is common to all expressions and is omitted. Note that $\gamma_i(st_p,st_j) = -\infty$ if there is no possible transition between states st_p and st_j.

During the forward recursion the parameter a_i is obtained on every recursion step i, $i = 0,\ldots,(N-1)$, through the whole trellis for every state st_j, $j = 0,\ldots,M^{K-1}$ according to the following equation:

$$a_i(st_j) = \max^*_{p=0,\ldots,M^{K-1}} \left(a_{i-1}(st_p) + \gamma_i(st_p, st_j)\right). \quad (11)$$

Maximum search is done over all of the states. The $\max^*(x,y)$ function is as follows:

$$\begin{aligned} &\max^*(x,y) = \max(x,y) + \ln(1+\exp(-|x-y|)), \\ &\max^*(x,y,z) = \max^*(\max^*(x,y),z). \end{aligned} \quad (12)$$

The log-MAP transforms to max-log-MAP algorithm if only max term is used in (12). The initial conditions are $a_0(st_j) = \ln(1/M^K)$, $j = 0,\ldots,M^{K-1}$, assuming equal probability for each state to be the starting one.

Similarly the backward recursion is done in the opposite direction for i, $i = N,\ldots,1$:

$$b_{i-1}(st_j) = \max^*_{p=0,\ldots,M^{K-1}} \left(b_i(st_p) + \gamma_i(st_p, st_j)\right). \quad (13)$$

The initial conditions are $b_N(st_j) = \ln(1/M^K)$, $j = 0,\ldots,M^{K-1}$.

Once parameters a_i and b_i are obtained the final a posteriori LLRs for every transmitted channel bit can be calculated. This is done on every step i, $i = 1,\ldots,N$ for each bit u_d^i, $d = 0,\ldots,(D-1)$ in a group of D channel bits, mapped to the i-th complex modulation symbol:

$$\begin{aligned} LLR(u_d^i) = &\max^*_{\substack{\{st_p,st_j\}_d \to 0,\\ p,j=0,\ldots,M^K-1}} (a_{i-1}(st_p) + \gamma_i(st_p,st_j) + b_i(st_j)) - \\ &\max^*_{\substack{\{st_p,st_j\}_d \to 1,\\ p,j=0,\ldots,M^K-1}} (a_{i-1}(st_p) + \gamma_i(st_p,st_j) + b_i(st_j)). \end{aligned} \quad (14)$$

In (14) the notation $\{st_p,st_j\}_d \to 0$ (or 1) means a transition which complies to the value 0 (or 1) for d-th bit. Thus the first max is done over all transitions for which $u_d^i = 0$, and the second max – over all transitions for which $u_d^i = 1$.

Based on (7) the proposed SEFDM demodulator tries to eliminate the main part of intersubcarrier interference in SEFDM-symbol but not all of it. This part of intersubcarrier interference grows with K producing lower BER at the cost of higher complexity (the number of states increases with K).

Note that the SEFDM demodulator also produces the extrinsic information of the following form [5]:

$$LLR_e(u_d^i) = LLR(u_d^i) - LLR_a(u_d^i). \quad (15)$$

In (15) $LLR_a(u_d^i)$ is the a priory information for bit u_d^i. These extrinsic LLRs are obtained through the knowledge of the trellis structure and can be used in iterative demodulation process.

IV. Proposed iterative SEFDM demodulator

The log-MAP algorithm for SEFDM-symbols demodulation/demapping described in the previous section produces LLRs for channel bits. Various FEC schemes are often used in wired and wireless telecommunication systems to detect and correct bit errors. In the case when a FEC scheme is used in concatenation with SEFDM modulation (Fig. 6) the following iterative SEFDM demodulator can be proposed (Fig. 7). Its structure is quite similar to turbo equalizer schemes.

The proposed iterative SEFDM demodulator consists of 4 parts: SEFDM demodulator, deinterleaver, MAP decoder for used FEC and interleaver. The extrinsic LLRs from SEFDM demodulator are deinterleaved and fed into the MAP decoder. The latter produces its own a posteriori LLRs $LLR^{dec}(u_d^i)$ and extrinsic LLRs $LLR_e^{dec}(u_d^i)$, which are interleaved and sent into the SEFDM demodulator as a priory information $LLR_a(u_d^i)$. This LLR flow constitutes one iteration. Several iterations are possible. The hard decisions from MAP decoder are taken out at the last iteration. All the MAP algorithms in the iterative scheme use extrinsic LLRs instead of the a posteriori LLRs to reduce the correlation between decisions on each iteration.

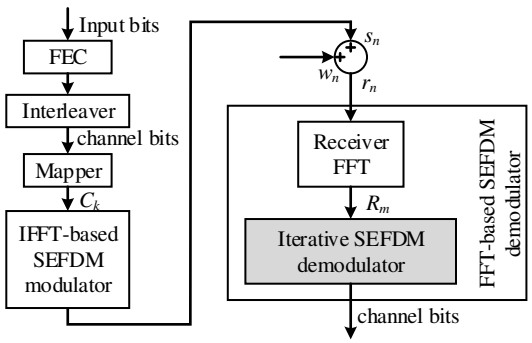

Fig. 6. System model for concatenation of FEC and SEFDM modulation

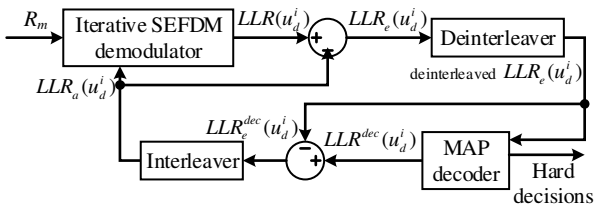

Fig. 7. Iterative SEFDM demodulator

Note that the log-MAP decoder on Fig. 7 has to provide LLRs for channel bits and hard decisions for information bits as well. The LLRs for channel bits are computed in a similar way as in (14).

V. Simulation results

Simulations of two proposed SEFDM demodulators (noniterative and iterative) were done in Matlab for QPSK modulation for various values of α, K and N. In all cases the AWGN channel was considered assuming perfect knowledge of noise power and perfect time and frequency synchronization. The confidence interval for all simulations is 0,99 given the confidence probability 0,1. We start with results for noniterative SEFDM demodulator and continue with those for iterative scheme.

At first BER performance of SEFDM demodulator for log-MAP and max-log-MAP algorithms is shown on the Fig. 8 (K = 3, 5, 7, $\alpha = 3/4$, $N = 200$, $N_{FFT} = 256$). It is clear to see that the difference between these two algorithms is negligible. Therefore, max-log-MAP is used in further simulations. In addition, the performance of maximum likelihood and simple FFT detection are shown (with notations ML and FFT respectively). In simple FFT detection scheme $\hat{C}_m = R_m$, $m = -N/2,\ldots,N/2-1$. Such scheme does not work even for quite good $\alpha = 3/4$. The performance of ML algorithm is shown only for small number of subcarriers $N = 10$ due to exhaustive search high computational complexity. The performance of SEFDM demodulator increases greatly as K grows.

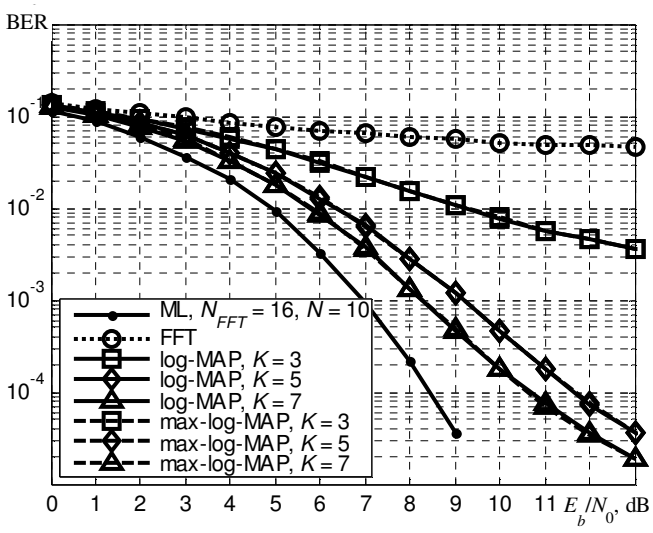

Fig. 8. BER performance of SEFDM demodulator for log-MAP and max-log-MAP algorithms, $K = 3, 5, 7$, $\alpha = 3/4$, $N = 200$, $N_{FFT} = 256$

The performance of SEFDM demodulator for various N is presented on Fig. 9 ($\alpha = 3/4$, $K = 7$). SEFDM with small N outperforms the one with large N, because of lower total level of intersubcarrier interference. For large E_bN_0 the decay rate of the curves on Fig. 9 slightly decreases. At high E_bN_0 the AWGN is quite small compared to the intersubcarrier interference. The latter comes to the fore requiring larger K values to effectively reduce the intersubcarrier interference level and demodulate SEFDM signals. The energy loss for BER = 10^{-5} is only 1 dB for $K = 7$ (relatively ML for $N = 10$).

The BER performance of SEFDM demodulator for various α is shown on the Fig. 10 (for $K = 5$, $N = 200$, $N_{FFT} = 256$). We can see that for low values of α BER is very high, several curves even saturate. As it was mentioned above the level of intersubcarrier interference grows as α decreases and for low values of α more subcarriers are to be taken in consideration in (7) for better BER performance. For $\alpha = 1/2$ the following notation for K is used: $K = 5(3)$. It means that for such α there is no difference between $K = 3$ and $K = 5$ because of the fact that $g_{-2} = g_2 = 0$ (Fig. 4b). Note that high BER for low α values is about 10^{-2} and less: this opens a good opportunity to reduce BER through a FEC in iterative schemes.

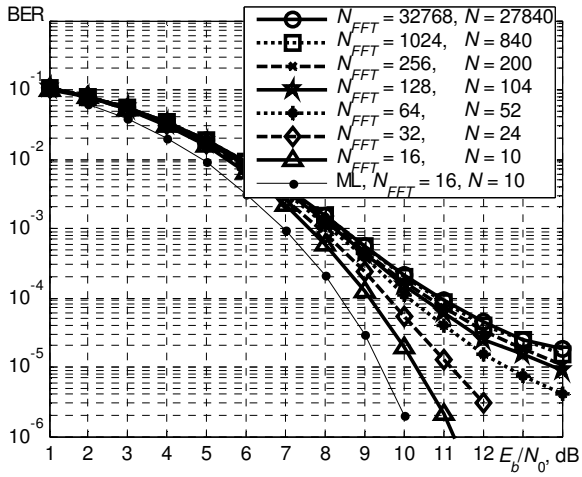

Fig. 9. BER performance of SEFDM demodulator for various N, $\alpha = 3/4$, $K = 7$

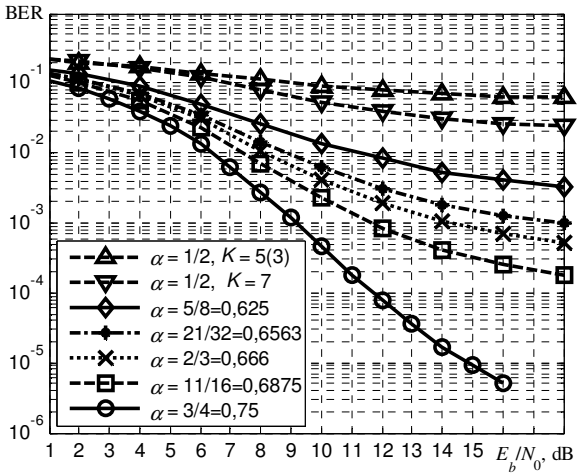

Fig. 10. BER performance of SEFDM demodulator for various α for $K = 5$, $N = 200$, $N_{FFT} = 256$

Now we move to the iterative SEFDM demodulator performance analysis. Remind that FEC and interleaver blocks have to be added at the transmitter (Fig. 6). In all simulation cases the max-log-MAP algorithm was used for FEC decoder, the code block size was ~2000 bits, the interleaving was done over one code block pseudo randomly. Simple convolutional code (3, [5 7]) with rate 1/2 was used.

The BER performance of iterative SEFDM demodulator for $\alpha = 3/4$ ($K = 3, 5$) and $\alpha = 1/2$ ($K = 5, 7$) is shown on Fig. 13 and Fig. 14 ($N = 200$, $N_{FFT} = 256$). The BER decreases greatly for iterative reception scheme. Moreover, no saturations for small α are present. We can see that only small number of iterations is enough to get reasonable BER performance gain: 2 iterations for $\alpha = 3/4$ and 3 iterations for $\alpha = 1/2$. Note that this result does not depend on the value of K.

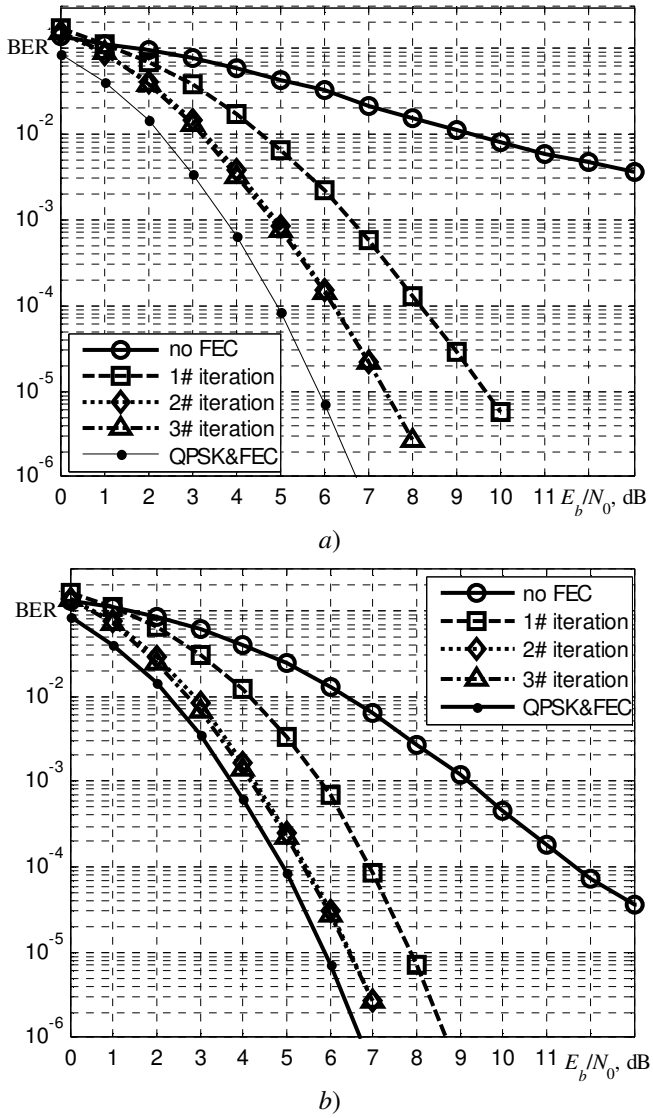

Fig. 11. BER performance of iterative SEFDM demodulator for $\alpha = 3/4$, $N = 200$, $N_{FFT} = 256$, *a*) $K = 3$; *b*) $K = 5$

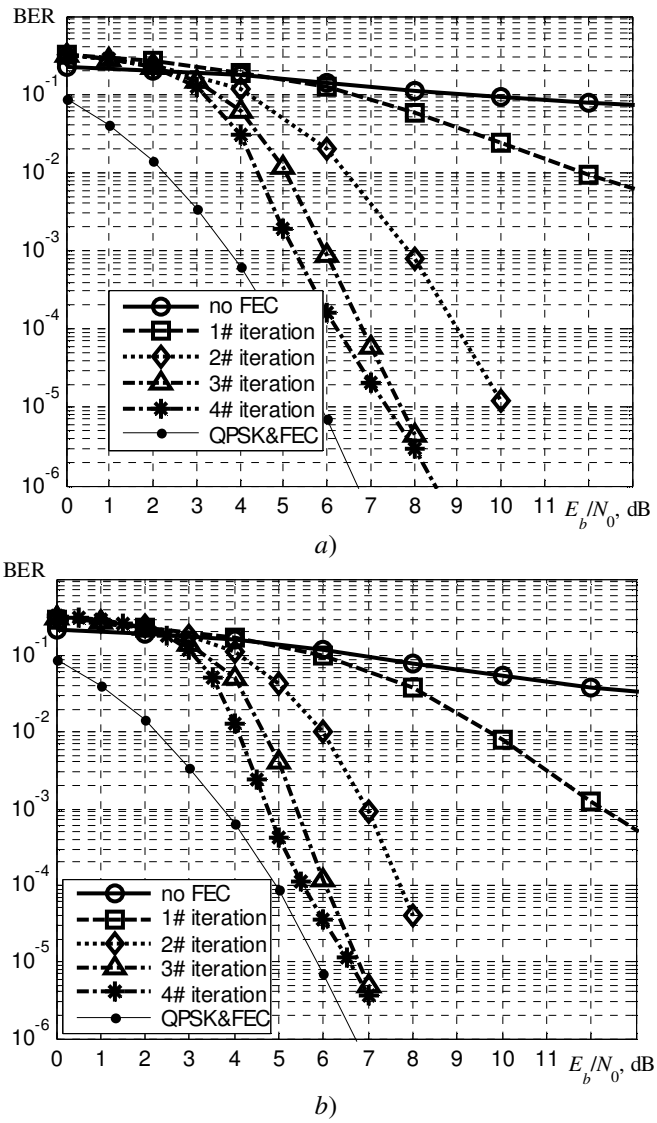

Fig. 12. BER performance of iterative SEFDM demodulator for $\alpha = 1/2$, $N = 200$, $N_{FFT} = 256$, *a*) $K = 3$; *b*) $K = 7$

The most important thing is that the BER performance of iterative SEFDM demodulator increases asymptotically towards the performance of pure single carrier QPSK&FEC scheme (with the same block size and max-log-MAP decoding algorithm implementation). Given $\alpha = 3/4$ the energy loss for BER = 10^{-5} is ~1,5 dB for $K = 3$ and ~0,5 dB for $K = 5$. Also for $\alpha = 1/2$ the energy loss for the same BER level is ~1,5 dB for $K = 5$ and ~0,7 dB for $K = 7$.

In other words, we have approximately the same performance of SEFDM modulation and of the classic QPSK modulation. However, the latter has $1/\alpha$ times worse spectral efficiency. The cost is higher computational complexity. For example, for $\alpha = 1/2$, $K = 7$ and QPSK modulation the SEFDM demodulator trellis has $4^{7-1} = 4096$ states.

VI. Conclusions

A new FFT-based trellis receiver for SEFDM signals is proposed. It includes FFT and the SEFDM demodulator or

iterative SEFDM demodulator (if FEC and interleaver are used). The proposed SEFDM demodulator can be applied to the signal with large number of subcarriers: the transition from 104 to 27840 subcarriers results in 1 dB loss for BER = 10^{-5} for $\alpha = 3/4$. Wherein the energy loss relative to maximum likelihood detection is no more than 2 dB (less than 1 dB for $K = 7$) for BER levels where no saturation effect is present. The performance of proposed iterative SEFDM demodulation is comparable with the one of classic coded QPSK modulation: the energy loss is only 0,7 dB for $K = 7$, $\alpha = 1/2$, $N = 200$ for BER = 10^{-5}. Very small number (2-3) of iterations is required to effectively demodulate SEFDM-symbol.

The main drawback of the proposed SEFDM demodulator is its intractable complexity for high order modulations (e.g. QAM-64). Further research have to be done to simplify the proposed algorithms.

REFERENCES

[1] Alexandr B. Kislitsyn, Andrey V. Rashich, Ngok Nuen Tan Generation of SEFDM-Signals Using FFT/IFFT // 14th International Conference, NEW2AN 2014 and 7th Conference, ruSMART 2014, Proceedings, 8638 LNCS

[2] Zavjalov S. V., Makarov S. B., Volvenko S. V., Balashova A. A. Efficiency of coherent detection algorithms nonorthogonal multifrequency signals based on modified decision diagram // 15th International Conference on Next-Generation Wired/Wireless Advanced Networks and Systems, NEW2AN 2015 and 8th Conference on Internet of Things and Smart Spaces, ruSMART 2015. – 2015.

[3] D. Dasalukunte, F. Rusek, and V. ¨Owall, "An iterative decoder for multicarrier faster-than-Nyquist signaling systems," in Proc. of IEEE International Conference on Communications (ICC), Cape Town, May 2010.

[4] I. Kanaras, A. Chorti, M. Rodrigues and I. Darwazeh, "Analysis of Sub-optimum detection techniques for a bandwidth efficient multi-carrier communication system," Proceedings of the Cranfield Multi-Strand Conference, Cranfield University, pp. 505-510, May 2009.

[5] A. Dejonghe, X. Jaspar, X. Wautelet and L. Vandendorpe, "Assessing the performance of turbo-equalized bit-interleaved turbo-coded modulation," in Proc. SCVT'2004 - IEEE Symposium on Communications and Vehicular Technology, Gent, Belgium, Nov. 9, 2004

[6] C. Douillard, M. Jezequel and C. Berrou, "Iterative correction of intersymbol interference: Turbo-equalization," Eur. Trans. Telecommun., vol. 6, no. 5, pp. 507–511, Sep.-Oct. 1995.